Cancer Chemotherapy and Pharmacology (2021) 87:327–336
https://doi.org/10.1007/s00280-020-04186-x

ORIGINAL ARTICLE

Irinotecan-induced intestinal mucositis in mice: a histopathological study

Thaise Boeing[1,2] · Marcelo Biondaro Gois[3] · Priscila de Souza[1] · Lincon Bordignon Somensi[1] · Débora de Mello Gonçales Sant´Ana[4] · Luisa Mota da Silva[1]

Received: 12 June 2020 / Accepted: 19 October 2020 / Published online: 31 October 2020

Abstract

Purpose Intestinal mucositis is an important adverse effect of antineoplastic therapy, which remains without adequate treatment. The present study aimed to carry out a complete evaluation of the histopathological changes during irinotecan-induced intestinal mucositis, using the protocol most found in the pharmacological reports nowadays to better understand irinotecan toxicity and support future studies on drug discovery.

Methods Intestinal mucositis was induced by treating swiss mice for 4 days with irinotecan (75 mg/kg, i.p.). After 72 h post irinotecan, the mice were sacrificed and the small intestine and colon were excised to performed histological analysis by stained tissue with hematoxylin/eosin (H&E).

Results Histoarchitecture loss, villus/crypt ratio reduction, atrophy of the muscular layer, hypertrophy in the submucosal and mucous layers, ruptures in the epithelium, as well as extent cellular infiltrate and presence of micro abscesses and the fusion of the crypts were observed in the histological analysis. Moreover, duodenum and colon had increased intraepithelial lymphocytes and mitotic figures. However, submucosal ganglia were decreased in the duodenum and increased in the colon.

Conclusions The data obtained in the present study provides new evidence that irinotecan-induced intestinal mucositis highly affects small intestine and colon, further contributing to establish criteria in light of the histopathological changes induced by irinotecan during intestinal mucositis and facilitating inter-study comparisons.

Keywords Chemotherapy · Morphometric analysis · Intraepithelial lymphocytes · Enteric ganglia · Villus · Crypts

Introduction

Intestinal mucositis is defined as damage to mucous membranes of the intestine resulting from direct damage to the division of epithelial cells and loss of renewal capacity induced by both anticancer chemotherapy and radiation therapy. Moreover, this condition is associated with a complex process involving all cells of the mucosa and systemic inflammatory response that culminates in structural, functional, and immunological changes in the gastrointestinal tract [1].

Among the drugs associated with the appearance of intestinal mucositis, irinotecan is of great clinical importance. This topoisomerase I inhibitor is used for the treatment of several solid tumors [2]. Since it was approved for the treatment of metastatic colorectal cancer and included in combination regimens with other drugs, it significantly increased the survival rate of patients [3]. Nevertheless, irinotecan is also among the main agents that cause intestinal mucositis and, therefore, associated with morbidity, increased hospitalization costs, palliative care, and frequent infections [4]. Common symptoms experienced by patients are nausea, vomiting, abdominal pain, bloating, and diarrhea [5].

In fact, irinotecan-induced diarrhea occurs in 60–80% of patients [6], often resulting in chemotherapy-dose reductions

✉ Thaise Boeing
tize.thaise@gmail.com

1 Pharmaceutical Sciences Graduate Program, Universidade do Vale do Itajaí, Rua Uruguai, 458, Itajaí, Santa Catarina, Brazil

2 School of Pharmaceutical Sciences of Ribeirão Preto, Universidade de São Paulo, Ribeirão Preto, São Paulo, Brazil

3 Federal University of Recôncavo of Bahia and Institute of Health Sciences, Universidade Federal da Bahia, Salvador, Bahia, Brazil

4 Department of Morphological Sciences, Universidade Estadual de Maringá, Maringá, Paraná, Brazil

and treatment delays or failures [7]. Once oral rehydration and pharmacological agents to decrease intestinal motility are the few treatments employed in clinical practice [8], many studies have seeking new therapeutic strategies for treatment, or even to prevent, the development of intestinal mucositis using animal models [9–13]. Indeed, histological changes, such as apoptosis, hypoproliferation of small and large intestines, and changes in goblet cells have been described [14, 15] after 2 days of irinotecan application at doses of 200 mg/kg (i.p). Thus, the present study aimed to carry out a complete evaluation of the histopathological changes during irinotecan-induced intestinal mucositis, using the protocol most found in the pharmacological reports (75 mg/kg, i.p. daily, for 4 days), to evaluate the tissue morphometry, but also the changes on the enteric ganglia, mitosis, and intraepithelial lymphocytes. A better understanding of irinotecan-induced toxicity may support the comprehension of new ways to improve preventive, diagnostic, or therapeutic strategies for the treatment of mucositis.

Materials and methods

Animals

Swiss female mice (25-30 g) were supplied by the animal facilities of the Universidade do Vale do Itajaí (UNIVALI), after approval by the institutional animal ethics committee (number 021/16p). The mice were housed under standard laboratory conditions (12-h light/dark cycle, temperature of 22 ± 2 ºC). All animal care and experimental procedures complied with international standards, following all the ethical guidelines on animal welfare.

Irinotecan-induced intestinal mucositis

The mice were divided into two groups of 6 animals each that received vehicle (VEH: Saline, 10 ml/kg, i.p.) or irinotecan (IRI, 75 mg/kg, i.p.) for 4 days to induce intestinal mucositis [16]. Mice were sacrificed 72 h after the last application of irinotecan or saline, in the CO_2/O_2 chamber. The small intestine and colon were excised, cleaned, and fixed in Alfac (85% ethanol 80%; 10% formaldehyde and 5% acetic acid) for 24 h. They were subsequently dehydrated with alcohol and xylene, embedded in paraffin wax, sectioned at 5 µm and stained with hematoxylin/eosin (H&E) for histopathological and morphometric analysis.

Histopathological analysis

Histopathological analysis was analyzed under a photonic microscope following the criteria described in previous studies [17, 18] with a few modifications.

The mucosal histoarchitecture loss score was considered as (0) normal histological findings; (1) slight focal or diffuse inflammation in the lamina propria, but with normal epithelium and mild edema and congestion; (2) moderate focal or diffuse inflammation, rupture of the epithelium, moderate edema and congestion in the mucosa and extremities of villi; and, (3) intense focal or diffuse inflammation, intense destruction of the epithelium, severe edema and moderate congestion, abscess formation in villi (if any) or crypts.

The extension of the cellular infiltrate score was considered as (0) no cellular infiltration; (1) discrete infiltrate present only in the mucosa; (2) moderate infiltrate present in the mucosa and submucosa; and, (3) severe infiltrate that involves mucosa, submucosa and muscle.

The epithelitis score was considered as (0) absent; (1) rare; (2) frequent and (3) very common leukocytes between epithelial cells.

To evaluate the villus/crypt ratio in the duodenum, the villus height (from villus tip to villus–crypt junction) and crypt depths (defined as invagination depth between adjacent villi) were measured.

The cryptitis score in the colon was considered as (0) absence; (1) discrete; (2) moderate and (3) intense inflammatory infiltrate in the crypts.

Morphometric analysis

Images captured with a digital camera (Olympus® SC30, 3.0 Megapixel) coupled to an optical microscope (Olympus® BX43F—Minato-Ku, Japan) were used for the measurements.

The thickness (µm) of the muscle, submucosa, mucosa, height, and width of villi (in the duodenum) and width and depth of the crypts were evaluated under 20 × magnification. The villus width was obtained from the average of three measurements taken at the base, middle third, and at the apex. Sixty-four measurements of each parameter were performed, with 16 measurements per quadrant of the duodenum and colon of all mice.

Images captured under 100 × magnification were used to measure the height and width (at three points) and the largest and smallest diameter of the nucleus of 80 enterocytes in the duodenum and colon of each mice. Measurements were performed using Image-Pro Plus 4.5.0.29 (Media Cybernetics Silver Spring, MD, USA).

Quantification of mitotic figures

Quantification of mitotic figures were performed in sixty-four crypts of each mouse, being 16 per quadrant were evaluated. The results were presented by an average of mitoses

per crypt. Quantification was performed directly under the photonic microscope (model CX31 Olympus) under 40 × magnification.

Quantification of intraepithelial lymphocytes (IELs)

Quantification of intraepithelial lymphocytes was performed in the tissue samples stained with H&E. The IELs of 2560 epithelial cells of the duodenum and the colon from each mouse were counted. The number of IELs/100 epithelial cells was calculated. Quantification was performed directly under the photonic microscope (model CX31 Olympus) under 40 × magnification.

Evaluation of the enteric nervous system (ENS)

The area (μm^2) of the myenteric plexus and submucosal plexus ganglia were evaluated under 40 × magnification. ten ganglia per mice from each plexus were measured in the duodenum and colon.

Data and statistical analysis

The data were expressed as mean ± standard deviation (SD) and *t* test was applied to evaluated differences between the groups. The non-parametric data were expressed as the median with interquartile range and analyzed by Mann–Whitney test to compare differences between the groups. Statistical analysis was performed using the software GraphPad Prism version 7.00 (GraphPad Software, La Jolla, CA, USA). Statistical significance was accepted when $p < 0.05$. The data were analyzed by an investigator blinded to the experimental conditions.

Results

Histopathological analysis of irinotecan-induced intestinal mucositis in mice

As shown in Fig. 1e, the duodenum of mice exposed to irinotecan suffered extensive damage when compared to the vehicle. Changes such as histoarchitecture loss and flattening of the mucosa, villus and crypts, severe extension of the cellular infiltrate, and vacuolar degeneration in the cytoplasm of enterocytes can be observed, suggesting hydropic degeneration and abscess formation.

Indeed, the score for the histoarchitecture loss of the duodenum was 2.0-folds higher than vehicle group (Fig. 1a). The villus/crypt ratio of the tissue decreased 79.3% compared to vehicle (3.6 ± 1.1 μm) (Fig. 1b) and the score of inflammatory infiltrate (Fig. 1c) was significative increased (3-folds), while the epithelitis remained similar between the groups (Fig. 1d).

The colonic tissue was also significantly disturbed by irinotecan, as shown in Fig. 2d. Changes such as histoarchitecture loss, atrophy of the muscular layer, hypertrophy in the submucosal and mucous layers, and ruptures in the epithelium are observed, as well as extent cellular infiltrate and presence of micro abscesses and the fusion of the crypts.

The score for the histoarchitecture of the colon was 2.5-folds higher than vehicle group (Fig. 2a). Cryptitis score increased 3.3-folds (Fig. 2b) and inflammatory infiltrate 2.4-folds compared to the vehicle (Fig. 2c).

The measurement of the strata of the gut is shown in Table 1. In the duodenum, the thickness of the mucosa decreased significative (53.7%) in the mice exposed to irinotecan compared to the vehicle, while submucosa and mucosa layers increased thickness by 76.5 and 155.7%, respectively. The villus height decreased 50.2%, while the width increased 53.9%. The crypt's depth and width increased by 105.8% and 85.1%, respectively, while the enterocytes size did not change, as well as the diameter of their nuclei.

Unlike the duodenum, the muscle layer in the colon of animals exposed to irinotecan showed no difference from animals in the vehicle group, but similar to duodenum, submucosa and mucosa thickness increased by 73.1% and 113.4%, respectively. On the other hand, crypts depth and width of irinotecan-group did not show a difference in comparison to the vehicle, but enterocytes showed decreased height (37.9%) and decreased width (34.1%) without differences in the diameter of their nuclei.

Intraepithelial lymphocytes number of mice under irinotecan-induced intestinal mucositis

The number of intraepithelial lymphocytes increased significantly in both, duodenum (75.9%) and colon (39.1%) of mice exposed to irinotecan compared to their respective vehicles (7.5 ± 1.5 and 6.9 ± 0.4 IELs/100 epithelial cells) (Fig. 3).

Mitotic figures number of mice under irinotecan-induced intestinal mucositis

As visualized in Fig. 4, the number of mitotic figures also increased significantly in both duodenum (70.2%) and colon (25.2%) of mice exposed to irinotecan compared to their respective vehicles (2.1 ± 0.8 and 3.1 ± 0.4 mitoses/crypt).

Morphometry of ENS from mice under irinotecan-induced intestinal mucositis

As shown in Fig. 5, the myenteric ganglia of duodenum and colon have similar profiles in animals exposed or not

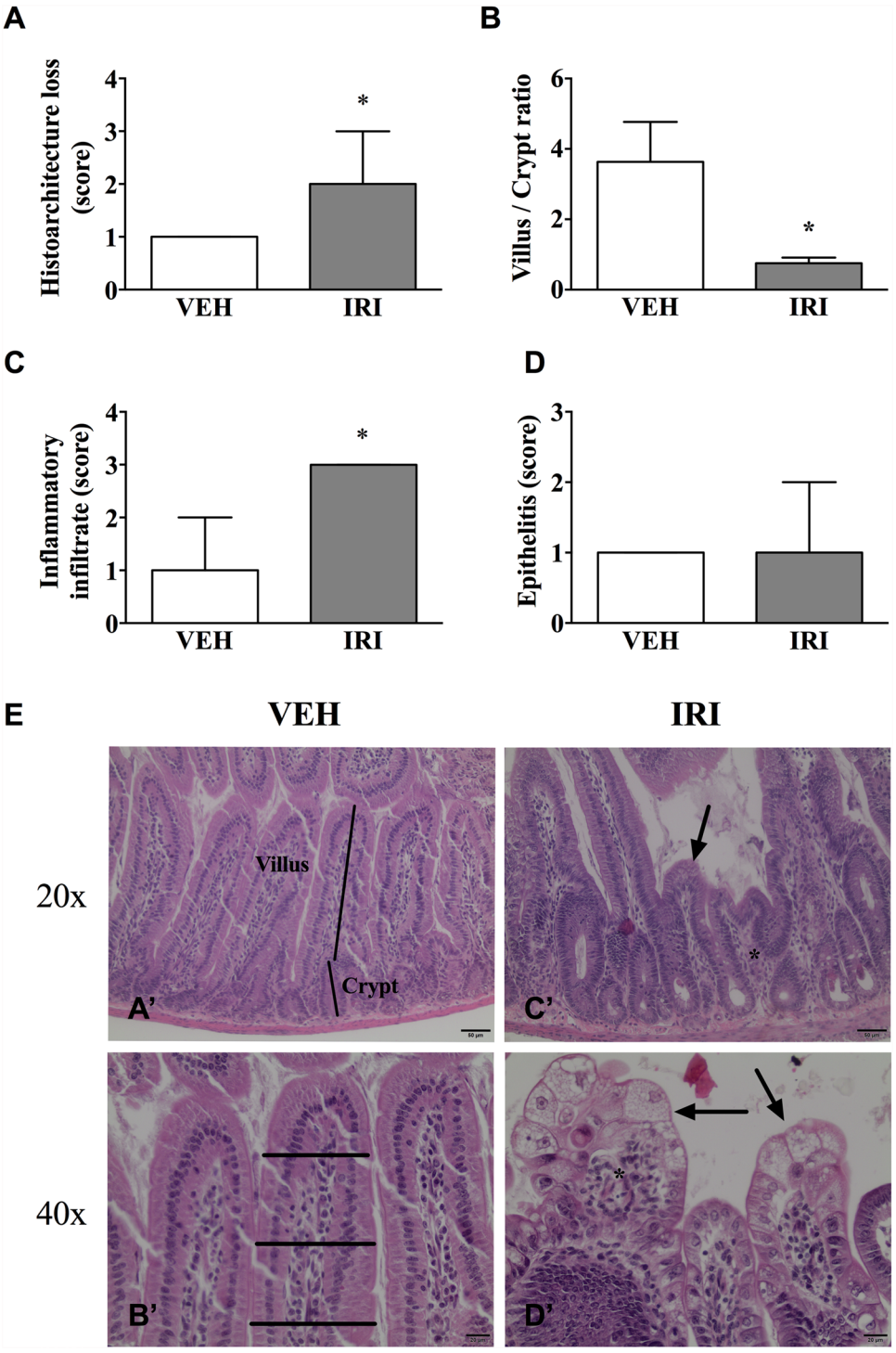

Fig. 1 Histopathology of duodenum. The mice received vehicle (VEH: Saline, 10 ml/kg, i.p.) or irinotecan (IRI, 75 mg/kg, i.p.) daily for 4 days to induce intestinal mucositis and were sacrificed 72 h after the last application of irinotecan or saline. **a** Histoarchitecture loss; **b** Villus/crypt ratio; **c** Inflammatory infiltrate; **d** Epithelitis. **b** The data were expressed as mean ± standard deviation (SD) and *t* test was applied to evaluated differences between the groups. The non-parametric data (scores) were expressed as the median with interquartile range and analyzed by Mann–Whitney test to compare differences between the groups. *$p < 0.05$ compared to VEH. **e** Photomicrographs of the duodenum wall stained by H&E. **a'** and **c'** Scale bar 50 µm; **b'** and **d'** Scale bar 20 µm. **a'** Villus height and crypts depth; (**b'**) Crypts width; (**c'**) Histoarchitecture loss and flattening of the mucosa (arrow) and severe extension of the cellular infiltrate (*). **d'** Vacuolar degeneration in the cytoplasm of enterocytes suggesting hydropic degeneration (arrows) and abscess formation

to irinotecan. However, submucosal ganglia of duodenum decreased by 42.5% in the irinotecan group compared to the vehicle (888.9 ± 125.3 µm), while in the colon this parameter increased in 43.5% (vehicle = 843.7 ± 189.3 µm).

Discussion

The classical signs of mucositis, including body weight loss and diarrhea, were observed after 72 h of the last intraperitoneal application of irinotecan (75 mg/kg, 4 days—data not shown). Chemotherapy-induced diarrhea appears to be a multifactorial process, including loss of intestinal

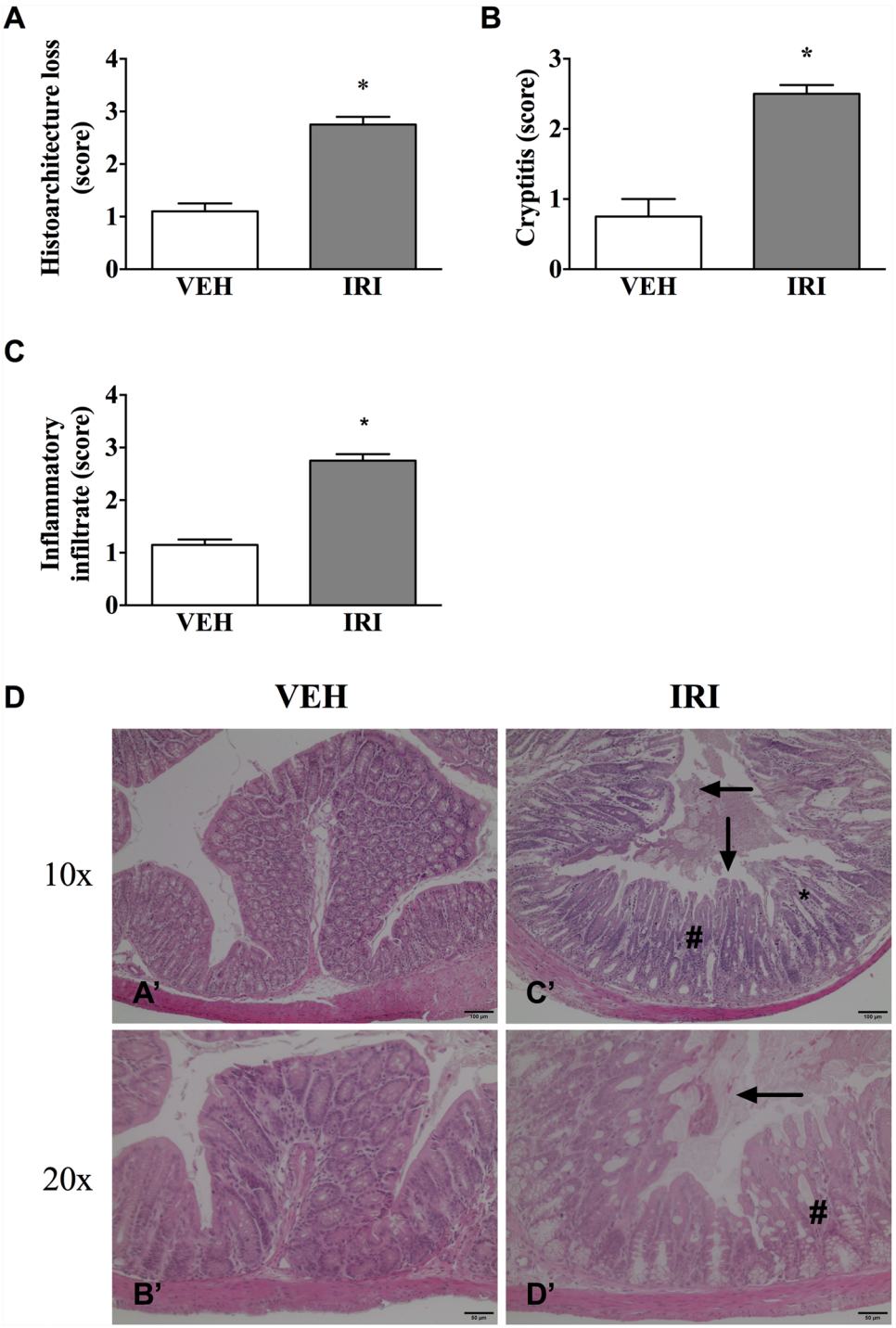

Fig. 2 Histopathology of colon. The mice received vehicle (VEH: Saline, 10 ml/kg, i.p.) or irinotecan (IRI, 75 mg/kg, i.p.) daily for 4 days to induce intestinal mucositis and were sacrificed 72 h after the last application of irinotecan or saline. **a** Histoarchitecture loss; (**b**) Cryptitis; (**c**) Inflammatory infiltrate. The data were expressed as the median with interquartile range and analyzed by Mann–Whitney test to compare differences between the groups. *$p < 0.05$ compared to VEH. **d** Photomicrographs of the colon wall stained by H&E. **a**' and **c**' Scale bar 100 µm; **b**' and **d**' Scale bar 50 µm. **a**' and **b**' Normal colonic tissue; **c**' and **d**' Histoarchitecture loss, atrophy in the muscular layer, hypertrophy in the submucosal and mucous layers and ruptures in the epithelium (arrows); extent of the cellular infiltrate (*); and presence of micro abscesses and the fusion of the crypts (#)

epithelium, superficial necrosis, and inflammation of the bowel wall [19]. In fact, morphometric changes in the duodenum, such as histoarchitecture loss and flattening of the mucosa, vacuolar degeneration in the cytoplasm of enterocytes suggesting hydropic degeneration and severe extension of the cellular infiltrate were observed. Ikuno et al. [16] also found marked shortening of the villi and epithelial vacuolation after 200 mg/kg of irinotecan-treatment (2 days), but mild infiltration of inflammatory cells. It is important to note that in the present study, cellular infiltrate was quantified by a score considering cellular infiltration in the mucosa, submucosa, and muscle layers, thus, even using a lower dose of irinotecan than the mentioned study, we have seen a more severe inflammatory cellular infiltrate. Besides, the chemotherapeutic did not induce epithelitis, which refers to the leukocytes between epithelial cells, demonstrating that

Table 1 Measurement of the strata of the wall of the duodenum and colon of mice exposed to irinotecan

Parameters (μm)		Duodenum	
		VEH	IRI
Muscular		70.85 ± 16.27	32.80 ± 8.29*
Submucosa	Thickness	28.81 ± 2.90	50.86 ± 15.94*
Mucosa		102.73 ± 36.31	262.75 ± 37.02*
Crypts	Depth	95.20 ± 27.15	196.00 ± 54.60*
	Width	33.69 ± 7.75	62.36 ± 15.57*
Villi	Height	324.90 ± 40.58	161.71 ± 12.64*
	Width	86.68 ± 14.79	133.42 ± 24.38*
Enterocytes	Height	33.08 ± 3.84	34.53 ± 9.03
	Width	6.28 ± 1.08	5.27 ± 1.60
Nuclei of the enterocytes	Largest-diameter	8.90 ± 1.06	10.19 ± 2.23
	Smallest-diameter	4.43 ± 1.35	4.48 ± 0.57
Parameters (μm)		Colon	
Muscular		62.40 ± 0.79	56.68 ± 14.19
Submucosa	Thickness	21.91 ± 7.08	37.93 ± 6.59*
Mucosa		189.51 ± 44.17	404.52 ± 60.48*
Crypts	Depth	127.87 ± 22.99	183.26 ± 61.13
	Width	41.76 ± 7.60	46.84 ± 7.55
Enterocytes	Height	30.57 ± 2.03	18.98 ± 1.14*
	Width	6.30 ± 0.84	8.45 ± 1.61*
Nuclei of the enterocytes	Largest-diameter	9.27 ± 1.63	8.98 ± 1.75
	Smallest-diameter	4.20 ± 0.84	5.06 ± 1.61

The mice received vehicle (VEH: Saline, 10 ml/kg, i.p.) or irinotecan (IRI, 75 mg/kg, i.p.) daily for 4 days to induce intestinal mucositis and were sacrificed 72 h after the last application of irinotecan or saline. The data were expressed as mean ± standard deviation (SD) and *t* test was applied to verify differences between the groups

*$p < 0.05$ compared to VEH

irinotecan-induced inflammation in mostly in the lamina propria and submucosa.

On the other hand, Ikuno et al. [16] have described morphologic changes in the colonic mucosa as minimal. In contrast, we have seen distinct histoarchitecture loss, atrophy of the muscular layer, hypertrophy in the submucosal and mucous layers and ruptures in the epithelium, as well as extent cellular infiltrate, and presence of micro abscesses and the fusion of the crypts in this tissue. In fact, colonic tissue presented a diffuse cellular infiltrate also in the crypts, as showed by cryptitis score. Thus, we provide histological evidence of the gravity of intestinal mucositis beyond small intestine, a data also supported by the biochemical findings of some studies, which have shown increased neutrophilic infiltration marker (MPO) and pro-inflammatory mediators such as TNF-α, IL-1β and IL-6 in the colonic tissue [9].

Another important novelty presented in this study was the increased number of intestinal intraepithelial lymphocytes (IELs) in the duodenum and colon of mice exposed to irinotecan. IELs comprise one of the most abundant T cell populations (belonging to both the T cell receptor-γδ (TCRγδ) + and TCRαβ + lineages) and potentially provide the first line of immune defense [20]. Tightly regulated of IEL function is crucial for the maintenance of the epithelial cell barrier and gut physiological inflammation [21]. Indeed, Fang et al. [22] showed that IL-10-producing CD4 + T cells were significantly suppressed in intestinal lamina propria of mice with mucositis, while Fernandes et al. [23] have shown that a higher frequency of Tregs was found, which was correlated with disease severity and diarrhea. Thus, the histological IEL overexpression observed in our data may have correlation with Treg enhance, despite this evidence, a limitation of our study is the lack of evaluation of the cell subtype.

Cytotoxic drugs are known to act by inducing apoptosis in cancer cells, but also adversely in intestinal crypts. This apoptotic process was reflected by the atrophy of the villus in the small intestine and by the damaged enterocytes in the colon, as well as by the increase in the number of mitotic cells observed in the crypts of both tissues at early time point (72 h after irinotecan), representing the beginning of the repair process after the damage induced by chemotherapy. Increased mitotic activity in female Dark Agouti rats was also observed at late time points, (96 h

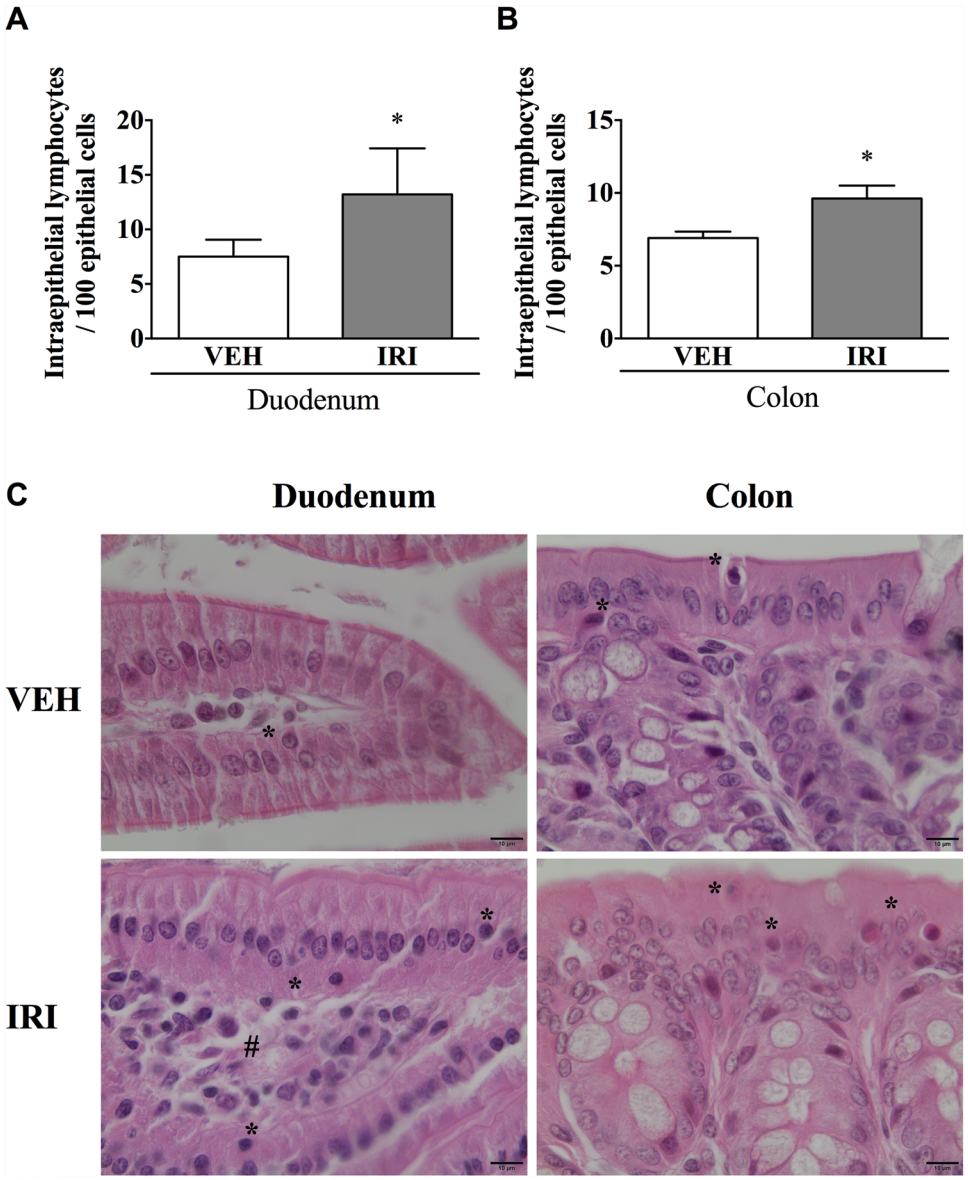

Fig. 3 Quantification of intraepithelial lymphocytes (IELs). The mice received vehicle (VEH: Saline, 10 ml/kg, i.p.) or irinotecan (IRI, 75 mg/kg, i.p.) daily for 4 days to induce intestinal mucositis and were sacrificed 72 h after the last application of irinotecan or saline. **a** IELs in the duodenum; **b** IELs in the colon. The data were expressed as mean ± standard deviation (SD) and *t* test was applied to evaluated differences between the groups. $*p < 0.05$ compared to VEH. **c** Photomicrographs of the tissues stained by H&E. Scale bar 10 µm. Distribution of IELs (*) in the epithelium. Note (#) the presence of leukocytes in the lamina propria of the IRI group

in the jejunum and 96–120 h in the colon) after damage induced by a single dose of irinotecan (200 mg/kg) [24].

A part of epithelial damage, the symptoms of intestinal mucositis are a consequence of a dynamic series of biological events involving different tissue compartments and mucosal cells [25]. The measurement of the strata of the wall of the duodenum and colon of mice exposed to irinotecan also confirm the extension of the damage at both sites. Although mucosa and submucosa layers had increased thickness, the muscular layer decreased in the duodenum. Boeing et al. [9] described that mice treated with irinotecan have decreased digestive motility rate probably in response to secretory diarrhea caused by the chemotherapeutic. By the data obtained herein, it is possible to suppose that loss of the muscle layer of the intestine wall can also be involved in this process, once gastric motility is regulated by the neural circuits that affect the activity of the smooth muscles [26].

Moreover, the enteric nervous system (ENS) is involved in regulating gut motility and secretion [27], in this way, we next evaluated the area of myenteric and submucosal plexus ganglia. Interestingly, irinotecan did not alter the myenteric ganglia of both duodenum and colon. Ikuno et al. [16] did not observe differences in the myenteric plexus of mice treated with irinotecan either, while Thorpe et al. [27] described a reduction of S-100 positive cells in the myenteric plexus of both tissues. On the other hand, the study developed by Thorpe et al. [27] detected a reduction in the number of S-100 positive cells in the submucosal plexus of the colon, while we found that submucosal ganglia profile was decreased in the duodenum but augmented in the colon of animals under intestinal

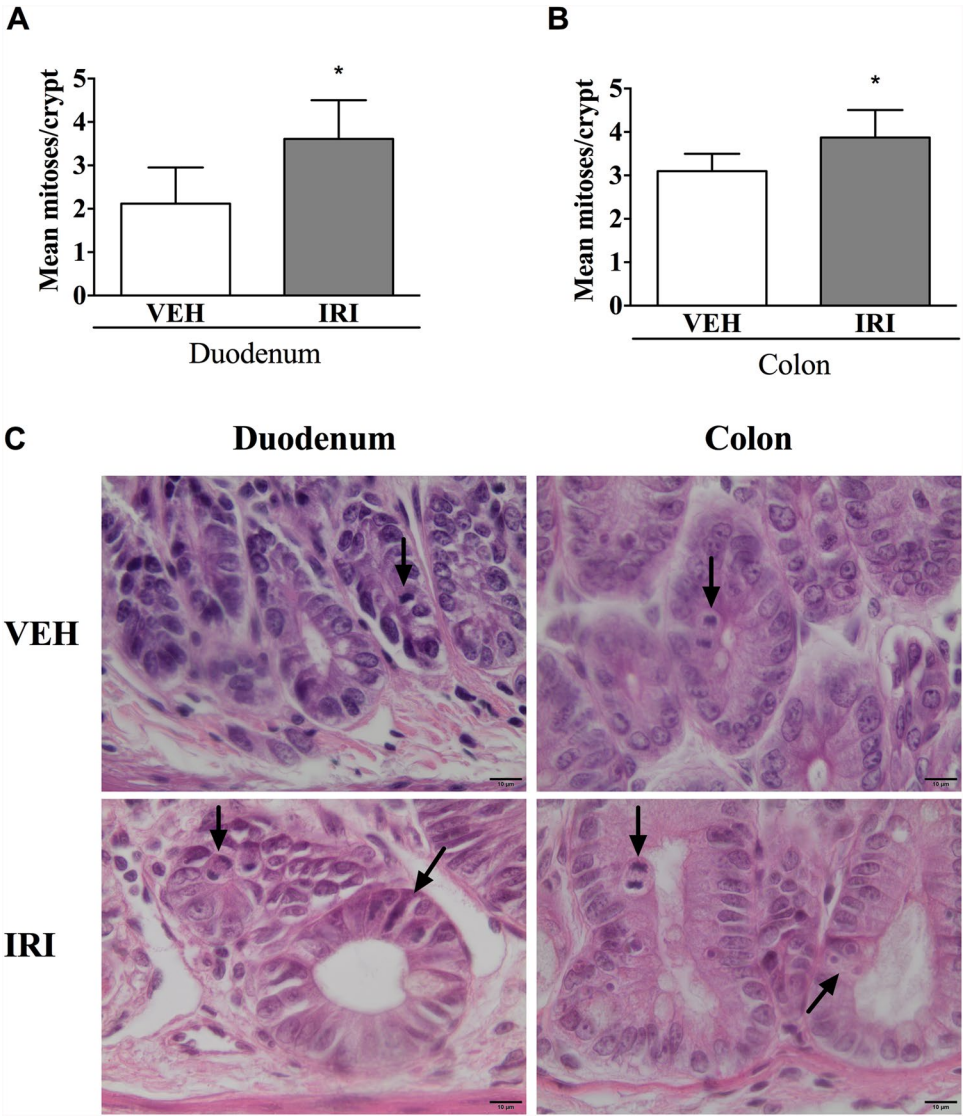

Fig. 4 Quantification of mitotic figures. The mice received vehicle (VEH: Saline, 10 ml/kg, i.p.) or irinotecan (IRI, 75 mg/kg, i.p.) daily for 4 days to induce intestinal mucositis and were sacrificed 72 h after the last application of irinotecan or saline. **a** Mitosis/crypt in the duodenum; **b** Mitosis/crypt in the colon. The data were expressed as mean ± standard deviation (SD) and *t* test was applied to evaluated differences between the groups. *$p < 0.05$ compared to VEH. **c** Photomicrographs of the tissues stained by H&E. Scale bar 10 µm. Mitotic figures (arrows) in the epithelium of intestinal crypts

mucositis which may contribute to some of the symptoms of mucositis relating to secretion. It is important to note that the mentioned study was carried out on Dark Agouti rats with a different protocol of intestinal mucositis induction, and the S100 antibody has previously been shown to detect other cells (e.g., neurons, glial cells, and Schwann cells), which may be responsible for the conflicting results.

Comparing intestinal histomorphology as assessed from H&E stained tissue sections from the same model in the hands of different researchers requires consistent criteria [18] thus, the data obtained in the present study, in addition to providing new evidence that irinotecan-induced intestinal mucositis highly affects the small intestine and colon, it establishes some histopathological changes that can be adopted as criteria to be evaluated in future studies, allowing to better explore new strategies for the treatment of mucositis.

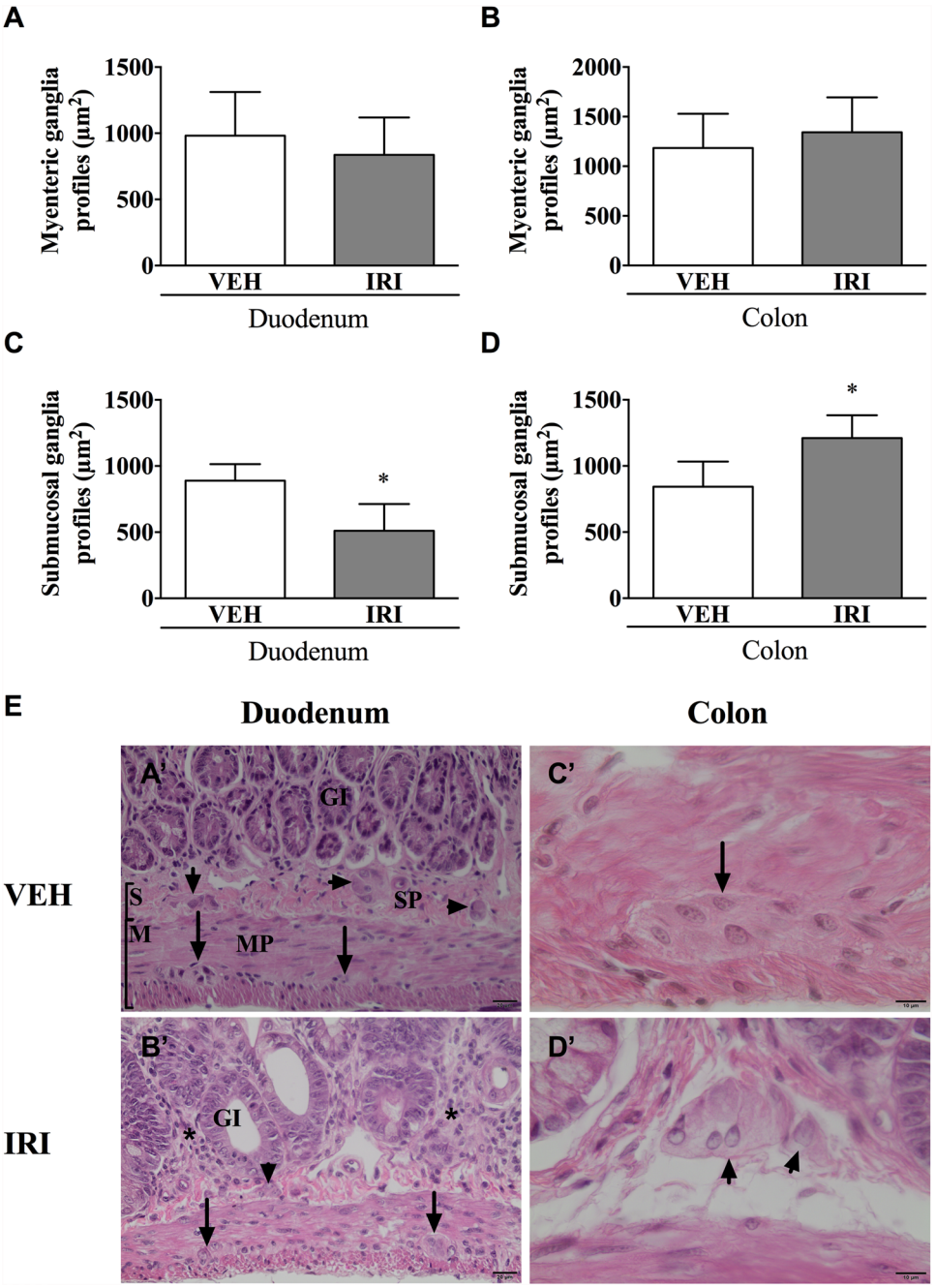

Fig. 5 Morphometry of the myenteric (arrows) and submucosal (arrow heads) plexus ganglia. The mice received vehicle (VEH: Saline, 10 ml/kg, i.p.) or irinotecan (IRI, 75 mg/kg, i.p.) daily for 4 days to induce intestinal mucositis and were sacrificed 72 h after the last application of irinotecan or saline. **a** Myenteric ganglia profiles of duodenum (μm^2); **b** Myenteric ganglia profiles of colon; **c** Submucosal ganglia profiles of duodenum (μm^2); **d** submucosal ganglia profiles of colon (μm^2). The data were expressed as mean ± standard deviation (SD) and *t* test was applied to evaluated differences between the groups. *$p < 0.05$ compared to VEH. **e** Photomicrographs of the tissues stained by H&E. **a**' and **b**' Scale bar 20 µm; **c**' and **d**' Scale bar 10 µm *S* submucosa; *M* muscular; *MP* myenteric plexus; *SP* submucosal plexus; *GI* Glands of Intestine or Crypts of Lieberkühn; Note (*) the large number of immune cells in the lamina propria, inflammatory infiltrate and atrophy of crypts

Acknowledgements We are grateful to the Coordenação de Aperfeiçoamento de Pessoal de Nível Superior (CAPES—Finance Code 001) and Conselho Nacional de Desenvolvimento Científico e Tecnológico (CNPq) for financial support, and to the University of Vale do Itajaí (UNIVALI) and State University of Maringá, where the study was carried out.

Author contributions TB, PS, and LBS performed the experimental work; MB and DMGSA performed the histological analysis; TB wrote the manuscript; LMS designed the study. All authors contributed to manuscript revision, read and approved the submitted version.

Funding Coordenação de Aperfeiçoamento de Pessoal de Nível Superior (CAPES—Finance Code 001) and Conselho Nacional de Desenvolvimento Científico e Tecnológico (CNPq). Dr. Thaise Boeing received a Postdoctoral scholarship from CNPQ.

Code availability Not applicable.

Compliance with ethical standards

Conflict of interest The authors have no conflicts of interest to declare.

Ethical approval License number (021/16p).

Consent to participate Not applicable.

Consent for publication All authors approved the submitted version of the manuscript and agree to publication of the material.

Availability of data and material Data is not publicly available, but can be provided on request.

References

1. Sangild PT, Shen RL, Pontoppidan P, Rathe M (2018) Animal models of chemotherapy-induced mucositis: translational relevance and challenges. Am J Physiol Liver Physiol 314:G231–G246. https://doi.org/10.1152/ajpgi.00204.2017
2. Rothenberg ML (1997) Topoisomerase I inhibitors: review and update. Ann Oncol Off J Eur Soc Med Oncol 8:837–855
3. Fujita KI, Kubota Y, Ishida H, Sasaki Y (2015) Irinotecan, a key chemotherapeutic drug for metastatic colorectal cancer. World J Gastroenterol 21:12234–12248. https://doi.org/10.3748/wjg.v21.i43.12234
4. Bajic JE, Johnston IN, Howarth GS, Hutchinson MR (2018) From the bottom-up: chemotherapy and gut-brain axis dysregulation. Front BehavNeurosci 12:104. https://doi.org/10.3389/fnbeh.2018.00104
5. Potten CS, Wilson JW, Booth C (1997) Regulation and significance of apoptosis in the stem cells of the gastrointestinal epithelium. Stem Cells 15:82–93. https://doi.org/10.1002/stem.150082
6. Vanhoecke B, Bateman E, Mayo B et al (2015) Dark Agouti rat model of chemotherapy-induced mucositis: establishment and current state of the art. Exp Biol Med 240:725–741. https://doi.org/10.1177/1535370215581309
7. Wardill HR, Gibson RJ, Van Sebille YZA et al (2016) Irinotecan-induced gastrointestinal dysfunction and pain are mediated by common TLR4-dependent mechanisms. Mol Cancer Ther 15:1376–1386. https://doi.org/10.1158/1535-7163.MCT-15-0990
8. Andreyev J, Ross P, Donnellan C et al (2014) Guidance on the management of diarrhoea during cancer chemotherapy. Lancet Oncol 15:e447–e460. https://doi.org/10.1016/S1470-2045(14)70006-3
9. Boeing T, de Souza P, Speca S et al (2020) Luteolin prevents irinotecan-induced intestinal mucositis in mice through antioxidant and anti-inflammatory properties. Br J Pharmacol 177:2393–2408. https://doi.org/10.1111/bph.14987
10. Alvarenga EM, Sousa NA, de Araújo S et al (2017) Carvacryl acetate, a novel semisynthetic monoterpene ester, binds to the TRPA1 receptor and is effective in attenuating irinotecan-induced intestinal mucositis in mice. J Pharm Pharmacol 69:1773–1785. https://doi.org/10.1111/jphp.12818
11. Cechinel-Zanchett CC, Boeing T, Somensi LB et al (2019) Flavonoid-rich fraction of *Bauhinia forficata* Link leaves prevents the intestinal toxic effects of irinotecan chemotherapy in IEC-6 cells and in mice. Phyther Res 33:90–106. https://doi.org/10.1002/ptr.6202
12. Arifa RDN, De PTP, Madeira MFM et al (2016) The reduction of oxidative stress by nanocomposite Fullerol decreases mucositis severity and reverts leukopenia induced by Irinotecan. Pharmacol Res 107:102–110. https://doi.org/10.1016/j.phrs.2016.03.004
13. Guo S, Gillingham T, Guo Y et al (2016) Secretions of bifiodobacteriuminfantis and lactobacillus acidophilus protect intestinal epithelial barrier function. J PediatGastroenterolNutr 64(3):404–412
14. Gibson RJ, Bowen JM, Inglis MRB et al (2003) Irinotecan causes severe small intestinal damage, as well as colonic damage, in the rat with implanted breast cancer. J Gastroenterol Hepatol 18:1095–1100. https://doi.org/10.1046/j.1440-1746.2003.03136.x
15. Logan RM, Gibson RJ, Bowen JM et al (2008) Characterisation of mucosal changes in the alimentary tract following administration of irinotecan: implications for the pathobiology of mucositis. Cancer Chemother Pharmacol 62:33–41. https://doi.org/10.1007/s00280-007-0570-0
16 Ikuno N, Soda H, Watanabe M, Oka M (1995) Irinotecan (CPT-11) and characteristic mucosal changes in the mouse Ileum and Cecum. JNCI 87:1876–1883
17. Taha AS, Dahill S, Nakshabendi I et al (1993) Duodenal histology, ulceration, and Helicobacter pylori in the presence or absence of non-steroidal anti-inflammatory drugs. Gut 34:1162–1166. https://doi.org/10.1136/gut.34.9.1162
18. Erben U, Loddenkemper C, Doerfel K et al (2014) A guide to histomorphological evaluation of intestinal inflammation in mouse models. Int J Clin Exp Pathol 7:4557–4576
19. Cherny NI (2008) Evaluation and management of treatment-related Diarrhea in patients with advanced cancer: a review. J Pain Symptom Manage 36:413–423. https://doi.org/10.1016/J.JPAINSYMMAN.2007.10.007
20. Cheroutre H, Lambolez F, Mucida D (2011) The light and dark sides of intestinal intraepithelial lymphocytes. Nat Rev Immunol 11:445–456
21. Hoytema van Konijnenburg DP, Reis BS, Pedicord VA et al (2017) Intestinal epithelial and intraepithelial T cell crosstalk mediates a dynamic response to infection. Cell 171:783-794.e13. https://doi.org/10.1016/j.cell.2017.08.046
22. Fang ZZ, Zhang D, Cao YF et al (2016) Irinotecan (CPT-11)-induced elevation of bile acids potentiates suppression of IL-10 expression. Toxicol Appl Pharmacol 291:21–27. https://doi.org/10.1016/j.taap.2015.12.003
23. Fernandes C, Wanderley CWS, Silva CMS et al (2018) Role of regulatory T cells in irinotecan-induced intestinal mucositis. Eur J Pharm Sci 115:158–166. https://doi.org/10.1016/j.ejps.2018.01.006
24. Stringer AM, Gibson RJ, Bowen JM et al (2009) Irinotecan-induced mucositis manifesting as diarrhoea corresponds with an amended intestinal flora and mucin profile. Int J Exp Pathol 90:489–499. https://doi.org/10.1111/j.1365-2613.2009.00671.x
25. Sonis ST (2004) The pathobiology of mucositis. J Neuropathol-ExpNeurol 4:277–284. https://doi.org/10.1038/nrc1318
26. Goyal R, Guo Y, Mashimo H (2019) Advances in the physiology of gastric emptying. Neurogastroenterol Motil 31:e13546
27. Thorpe D, Butler R, Sultani M et al (2019) Irinotecan-Induced mucositis is associated with goblet cell dysregulation and neural cell damage in a tumour bearing da rat model. PatholOncol Res. https://doi.org/10.1007/s12253-019-00644-x